IET Circuits, Devices & Systems

Research Article

IET Journals
The Institution of Engineering and Technology

Contactless power transmission for NFC antennas in credit-card size format

ISSN 1751-858X
Received on 17th January 2015
Revised on 16th December 2015
Accepted on 9th February 2016
doi: 10.1049/iet-cds.2015.0023
www.ietdl.org

Christopher A. Tucker[1] ✉, *Ulrich Muehlmann*[2], *Michael Gebhart*[3]

[1]*Cartheur Robotics spol. s r.o., Prague, Czech Republic*
[2]*NXP Semiconductors Austria GmbH, Gratkorn, Austria*
[3]*NXP Semiconductors Austria GmbH, Gratkorn Austria and Graz University of Technology, Graz, Austria*
✉ *E-mail: cartheur@gmail.com*

Abstract: Wireless energy transmission is a key element in Contactless HF Communication Technologies, such as radio frequency identification or near field communication (NFC). This power aspect differentiates the technology from conventional wireless communication. The authors consider the circuit model as a lumped-element description with a coupled-transformer field model to formulate a representation of the problem and include the orientation of the magnetic field in planar space. The authors propose a novel computational model to reveal the dynamics of energy transfer can be represented as a set of forces projected by the oscillator at the interface of free-space. Finally, a high-frequency finite-element simulation based on the authors' model is used to solve a practical problem of two coupled elliptical spiral-loop antennas of a credit-card size, where the authors consider their contribution in the context of NFC.

1 Introduction

Contactless communication has gained considerable practical importance over the last two decades. This is demonstrated by a billion dollar market today. Initially, this type of communication was different for close coupling at distances <10 mm, proximity at distances <10 cm, and vicinity at distances of 1 m, all operating at the high frequency carrier of 13.56 MHz. As applications evolved in the context of cards, standardisation was established, and loop antenna form-factors originally were related to the credit-card size shown in Fig. 1, specified as ID-1 format in ISO/IEC 7810.

Many aspects of the higher-layer protocol are related to the Contact IC Card specification family of ISO/IEC 7816. A contactless reader is the master and initiator of the communication to a battery-less card, providing supply power via an *H*-field alternating at a continuous wave carrier frequency, and a bi-directional data interface represented by a modulation of the carrier frequency. An additional requirement for power transmission combined to the data interface is the main difference of contactless communication against conventional wireless communication.

The power and signal air interface is specified in detail by the base standard for Close Coupling [1], Proximity [2], and Vicinity [3] systems. In the last few years, close coupling systems have disappeared from the market, replaced by near field communication (NFC) which is rapidly dominating the market. The NFC specification is provided by the NFC Forum [4] and covers the family of Proximity and Vicinity Standards, so it includes several protocols and modulation formats. The NFC interface is implemented in personal mobile devices like smartphones or tablet PCs which can then be used for access, authentication, ticketing, or payment applications in the existing contactless reader infrastructure. The different environments of these devices means necessary changes to the hardware, e.g. smaller loop antennas on ferrite materials for magnetic shielding, although the target is to achieve full interoperability with existing infrastructure.

More and more applications require a change in the antenna size for NFC tags or cards, or a change from simple rectangular planar spiral coil geometries to more complex shapes. As antenna design not only has the requirement to meet certain equivalent circuit element values, e.g. a certain inductance to meet a contactless card resonance frequency specification, but also a certain contactless performance, e.g. *H*-field or power specification required by the standards, there is a trend to use finite-element method (FEM) software instead of simple analytical formulas. In fact, there are many commercial, but also open source packages for this kind of simulation available, which an application engineer might use to design an NFC antenna.

A deeper understanding of the theoretical concepts, assumptions, and frame conditions will make such an NFC solution development process much more efficient as the technology evolves. Owing to the particularity of the NFC setup, there are advantages to frame the computation in the context of forces and the vector potential because of the dependency upon the interface of the antenna at free-space given possible complex geometries following the diversity available to the application. Therefore, models such as coupling by self and mutual inductances only explain a part of the story. The paper is organised as follows:

(i) To introduce the problem, we give a simple practical circuit-based description of two coupled loops as idealised transformer;
(ii) We then consider theoretical modelling of the transmission of energy as a function of the properties of the coupled loops, including translation to energy assumptions contained in the field model;
(iii) Finally, we solve a typical problem, following from the theory, for two Class 1 antennas in ID-1 Credit-Card format using FEM simulation software and compare these results with energy predicted by the theory.

It is the aim of the paper to demonstrate the coupling of the field is based more upon the forces consisting it – in terms of forward and reverse feedback – which can be manipulated for improvements of transmission efficiency. It is used to illustrate Larmor's contention and set a means to collect the terms for the vector potential, the *u*, *v*, and *w*, coordinates of the $\boldsymbol{A}$-vector from Maxwell [5]. Considering the theory for contactless power transmission by inductive loop antennas in the reactive near-field, we exclude resonant circuit considerations, except only to represent them in

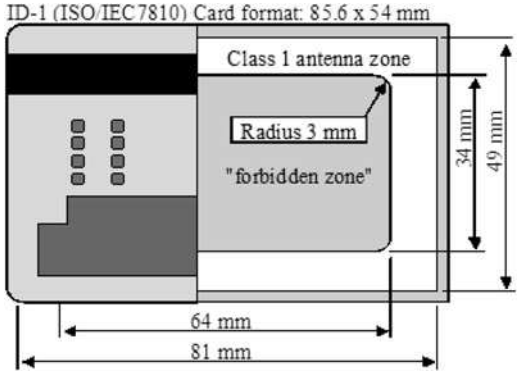

Fig. 1 *Credit-card format with optional card features*

the time domain, and focus on how energy is transmitted from the primary reader loop to the secondary card loop.

2 Circuit-based description of the model

If we consider energy transmission as a near-field coupling phenomenon of two planar loop coils, we can model a lossless inductive transformer to introduce the problem in the simplest way. We only consider magnetic coupling and the field behaviour exhibited at the interface of free-space while, in principle, neglecting losses in the form of off-resonances or any other parasitic effects. Inductances shall be linear and time-invariant. The idealised transformer is given in the schematics of Fig. 2, where we use the consecutive arrow system.

We would like to account for a small, yet significant amount of energy oscillating in the secondary circuit as a result of the coupling, and specifically, though not directly addressed, its coupled mode [6]. In terms of the energy in the magnetically coupled circuit, we denote the coil flux signal $\psi(t)$ for both branches. The coil flux is then given by the following equation

$$\begin{aligned}\psi(t) &= \varphi(t)n \\ &= \boldsymbol{B}(t)An,\end{aligned}$$

where φ is the magnetic flux, n the number of coil turns, $\boldsymbol{B}$ is the magnetic flux density, and A is the coil area. In order to divide the flux in this manner, we need to assume $\boldsymbol{B}$ is constant and oriented perpendicular to the area of the coil winding. Therefore, the branches are

$$\begin{aligned}\psi_1(t) &= L_{11}I_1(t) - L_{12}I_2(t), \\ \psi_2(t) &= L_{22}I_2(t) - L_{21}I_1(t),\end{aligned} \tag{2}$$

where L_{11} and L_{22} are the self-inductances of each coil, which we denote L_1 for the primary coil and L_2 for the secondary coil. L_{12} is equal to L_{21}, the counter-inductance or reflective mutual inductance, which we denote as M_{21} with the following stipulation that L and M are exclusively related to the conductor geometry of the antenna. The notation with M_{12} denotes the apparent value of

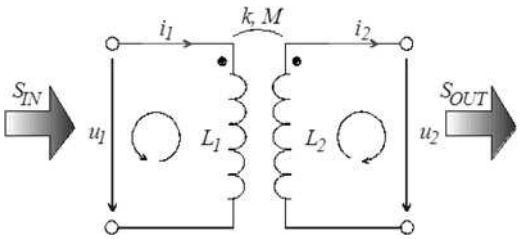

Fig. 2 *Idealised inductive transformer circuit*

the total value of M. Ordinarily, a way to determine M is to use the double integral Neumann formula [7]. Inductance, L, is determined in a similar way by using analytical formulas for basic geometries [8]. The derivation of the coil flux over time equals an induced voltage u_i. For harmonic sine wave signals, we exchange the derivation over time $(\mathrm{d}/\mathrm{d}t) \rightarrow \mathrm{j}\omega_0$, where ω_0 is the angular frequency, for the root-mean-square of U and I as $U(t)$ and $I(t)$. This returns the network equations

$$\begin{aligned}U_1 &= \mathrm{j}\,\omega_0 L_1 I_1 - \mathrm{j}\omega_0 M_{21} I_2, \\ U_2 &= \mathrm{j}\,\omega_0 L_2 I_2 - \mathrm{j}\,\omega_0 M_{12} I_1.\end{aligned} \tag{3}$$

The amount of flux originating from the primary coil not passing the secondary coil and equal the amount of flux originating from the secondary coil not passing the primary coil, is represented as the stray factor, σ, given by the following equation

$$\sigma = \frac{L_1L_2 - M_{12}^2}{\sqrt{L_1L_2}} = 1 - \frac{M_{12}^2}{L_1L_2} = 1 - \kappa^2. \tag{4}$$

The amount of flux of the primary coil passing through the secondary coil (and vice-versa) is represented as the coupling factor κ

$$\kappa = \frac{M_{12}}{\sqrt{L_1L_2}}. \tag{5}$$

If we assume the ideal transformer has no load ($I_2 = 0$), the induced voltage on the secondary side, from (3), results

$$U_2 = \mathrm{j}\,\omega_0 M_{12} I_1 = \mathrm{j}\,\omega_0 I_1 \kappa \sqrt{L_1L_2}, \tag{6}$$

measured by a contactless current probe. The above consideration shown is well-known for contactless system estimations, if the secondary current (of a card or tag) is considered negligibly small, e.g. for Vicinity systems. We argue that additional terms need to be considered as the physical systems become sufficiently small, as voltage and current become more significant. Under such a consideration, determination of the values κ and M can be difficult since it is easy to neglect actions on the conductor of an antenna at the interface of free-space. Traditionally, these quantities have been expressed purely in terms of geometry [8]. So, we offer the consideration used in a different fashion. If the primary and secondary inductances are known, the measurement of primary and secondary AC voltages allows the computation of coupling or mutual inductance of a coil arrangement. This approach [9] was also used to measure the coupling of the coils shown in Fig. 4.

The circuit-based approach of Fig. 2 also allows consideration of contactless power transfer from primary to secondary side, e.g. from reader to card. To do so, we consider a load impedance Z_L, which defines the relation of secondary voltage U_2 to secondary current I_2. This allows substitution of U_2 in (3), so

$$\begin{aligned}I_2Z_\mathrm{L} &= U_2 \\ &= \mathrm{j}\,\omega_0 L_2 I_2 - \mathrm{j}\,\omega_0 M_{12} I_1,\end{aligned} \tag{7}$$

where we can relate the secondary current as function of primary current as follows

$$I_2 = -\frac{\mathrm{j}\omega_0 M_{12}}{Z_\mathrm{L} - \mathrm{j}\omega_0 L_2} I_1. \tag{8}$$

Now, relating the primary voltage to primary current, using (3), as

$$U_1 = \left[\mathrm{j}\omega_0 L_1 + \frac{\omega_0^2 M_{12}^2}{Z_\mathrm{L} - \mathrm{j}\omega_0 L_2}\right] I_1, \tag{9}$$

we can calculate the apparent primary power S_IN and secondary

power S_{OUT} as follows

$$S_{\mathrm{IN}} = U_1 I_1^2 = \left[\mathrm{j}\omega_0 L_1 + \frac{\omega_0^2 M_{12}^2}{Z_{\mathrm{L}} - \mathrm{j}\omega_0 L_2}\right] I_1^2,$$
$$S_{\mathrm{OUT}} = I_1^2 Z_{\mathrm{L}} + \left(\frac{\mathrm{j}\omega_0 M_{12} - M_{21}}{Z_{\mathrm{L}} - \mathrm{j}\omega_0 L_2}\right)^2, \quad (10)$$

where the last term in (10) is extra apparent power held in the oscillating forces, subject to radiative losses the further the distance from the surface of the coil. Discussed in detail in Section 3, the terms of mutual inductance for the primary to secondary coupling, M_{12} the mutual inductance for the reflective secondary to primary coupling M_{21} is collected as a total mutual inductance, M_{Total} for convenience. The total apparent power contains the extra quotient plus the effective and reactive power. Together they are a description of the energy moving in the network due to forces in the oscillator exchanged at the interface between the antenna and free-space. Energy transfer, in this manner, can now be considered by the ratio of secondary output per primary input apparent power and the interface, which is (see (11))

Even if we assume negligible secondary current meaning very high impedance Z_{L}, there still remains a secondary voltage and an associated current over the inductance. Again, this scenario is similar to Vicinity systems. The apparent power will be only reactive, however, and this is also the case for the primary. We can reorder (10) to find

$$\frac{S_{\mathrm{OUT}}}{S_{\mathrm{IN}}}\Big|_{\mathrm{for} I_2 \ll} = \left|\frac{-I_1^2 \mathrm{j}\omega_0 M_{\mathrm{Total}}}{I_1^2 \mathrm{j}\omega_0 L_1}\right| \rightarrow \frac{M_{\mathrm{Total}}}{L_1} = \kappa\sqrt{\frac{L_2}{L_1}} = \frac{\kappa}{T}, \quad (12)$$

where T is the voltage transformation ratio (U_2/U_1). To consider effective power transmission, we need to consider the real part $P = \mathrm{Re}[S]$ for both input and output. Such a choice would then also involve the connected network, which is out of scope of this paper. Nevertheless, such a description is contained as power transfer for circular coils of an arbitrary orientation in space including the network [10]. As we assume the secondary current to be zero, there is no effect on the primary side where the current originates. Nevertheless there is reactive power transfer, and the amount is depending on the coupling factor, transformation ratio, and the choice of map of the forces in the vector potential field.

3 Theory of energy forces in the media

Following the circuit model of the previous section, a discussion of what constitutes the forces of the dynamic movement of energy is necessary as they contribute to quantities in the circuit itself. The novel contribution here is the inclusion of force towards prediction in stored energy, rather than anticipating their inclusion when computing self and mutual inductances, which are purely geometric. The discussion here quantifies the influence of forces across the field responsible for inductive coupling. The self and coupled inductance regions and their relation in space relative to the antenna described in the previous section are shown in Fig. 3.

The strength is restricted to areas in r. The length of d depends on the coupling factor, κ. When a current is applied, radial contributions contribute to the assumption of uniformity in the space at constant pressures and temperatures. The intensity of $\boldsymbol{B}$ is projected along d as $\boldsymbol{B}_z$, with a force. The material framework per unit volume is a force

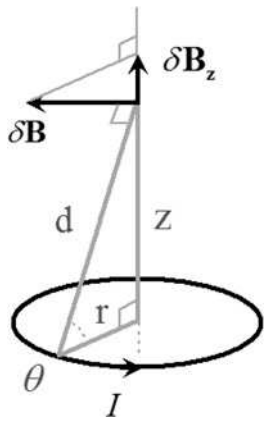

Fig. 3 *Identification of field geometry of a given loop*

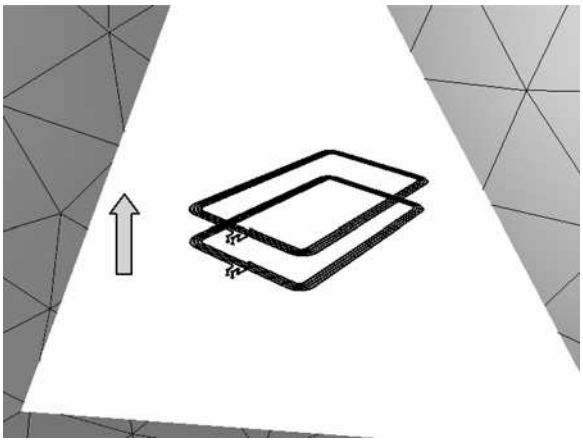

Fig. 4 *Meshed antenna setup inside a 50 × 50 × 50 cm air cube where the vertical arrow illustrates the z-dimension displacement for coupling determination*

$$\begin{pmatrix} u\frac{\mathrm{d}F}{\mathrm{d}x} + v\frac{\mathrm{d}G}{\mathrm{d}x} + w\frac{\mathrm{d}H}{\mathrm{d}x}, \\ u\frac{\mathrm{d}F}{\mathrm{d}y} + v\frac{\mathrm{d}G}{\mathrm{d}y} + w\frac{\mathrm{d}H}{\mathrm{d}y}, \\ u\frac{\mathrm{d}F}{\mathrm{d}z} + v\frac{\mathrm{d}G}{\mathrm{d}z} + w\frac{\mathrm{d}H}{\mathrm{d}z} \end{pmatrix}, \quad (13)$$

and a couple

$$(vH - wH,\ wF - uH,\ uG - vF), \quad (14)$$

from a rotational virtual displacement of the elements. In the case of the Ampère-Maxwell, there should simply be a force at right angles to the current

$$(vc - wb,\ wa - uc,\ ub - va), \quad (15)$$

forming its contextual sets of coordinates

$$\left\{-w\left(\frac{\mathrm{d}F}{\mathrm{d}z} - \frac{\mathrm{d}H}{\mathrm{d}x}\right),\ w\left(\frac{\mathrm{d}H}{\mathrm{d}y} - \frac{\mathrm{d}G}{\mathrm{d}z}\right),\ 0\right\}, \quad (16)$$

constrained by the geometry. In terms of force, Larmor [11] argues it

$$\frac{S_{\mathrm{OUT}}}{S_{\mathrm{IN}}} = \frac{\omega_0 M_{\mathrm{TOTAL}} Z_{\mathrm{L}}}{\omega_0\left(2L_1 L_2 Z_{\mathrm{L}} + M_{12}^2 Z_{\mathrm{L}}\right) + \mathrm{j}\left[L_1 Z_{\mathrm{L}}^2 + \omega_0^2\left(L_2 M_{12}^2 + L_1 L_2^2\right) + \left(L_1 M_{21}^2\right)\right]}. \quad (11)$$

differs from Ampere-Maxwell by the following equation

$$\begin{aligned}&\text{a force}\left(u\frac{\mathrm{d}F}{\mathrm{d}z}, v\frac{\mathrm{d}G}{\mathrm{d}z}, w\frac{\mathrm{d}H}{\mathrm{d}z}\right),\\&\text{and a couple}\,(-wG,\, wF,\, 0),\end{aligned}\tag{17}$$

to the equivalency of effective and reactive energy forces acting on the ends of each linear current element, as

$$F_{\mathrm{R}} = (uF,\, vG,\, wH),\tag{18}$$

per unit of cross-section, positive and the front and negative at the rear. Therefore, the internal stresses are homeostatic for each circuital current and do not disturb the resultant force on the conductor due to the presence of the field, however, when unbalanced appear as a quantity of directional energy. Since the symmetry of the space consisting the interior of the loop and that the loop is treated as a unit-circle, as

$$\delta \boldsymbol{B}_z = \frac{r}{d}\frac{\mu_0 I_0}{4\pi d^2}\delta s.\tag{19}$$

while the field is at any given point

$$\boldsymbol{B} = \frac{\mu_0 I_0}{2r}\cos(\theta),\tag{20}$$

given the potential at the boundary of the antenna. The magnetic vector decomposition is useful to describe field potential between ψ_1 and ψ_2 shaping the field geometry, consequently effecting its resonant linking to other coupled-modes [12, 13]. The model argues the fitting of temporal dynamics resulting from the forces in the field onto the magnetic vector potential $\boldsymbol{A} = (A_x,\, A_y,\, A_z)$ to construct a finite solution by casting, $\boldsymbol{A}_{\mathrm{t}}$ as the dot product of the tangent force vectors, as

$$\boldsymbol{A}_{\mathrm{t}} = A_{t_x}\cdot t_x + A_{t_y}\cdot t_y + A_{t_z}\cdot t_z.\tag{21}$$

The magnitude is relative to the stored energy at the interface of the conductor to free-space. The antenna carries a complex current from the oscillator, $I(t) = I_0\cos\omega t$, which is confined to the loop near its surface. The voltage is distributed across two synchronous yet differentiated time domains, separated by the notion of family time [14], indicating the scalar potential of the strain between the antenna and its interface at free-space. Therefore, individually, the form of the current is represented by the vector potential [15] of the loop as

$$\boldsymbol{A}(r) = \frac{\mu_0 \boldsymbol{I}}{4\pi}\oint_\ell \frac{\mathrm{e}^{-\mathrm{j}\kappa r'}}{r'}\mathrm{d}l',\tag{22}$$

where $\boldsymbol{I} = I_0\cos\omega_0$, is the complex current in the frequency domain. To simplify the appearance of the harmonic current in the following equations, it is expressed as

$$\boldsymbol{I} = \boldsymbol{u}_\gamma.\tag{23}$$

The evaluation of the potential depends of the location where $\mathrm{d}l'$ is being observed in the experiment. Expansion of the exponential form

$$\begin{aligned}\mathrm{e}^{-\mathrm{j}\kappa r'} &= \mathrm{e}^{-\mathrm{j}\kappa r}\mathrm{e}^{\mathrm{j}\kappa(r-r')}\\&\simeq \mathrm{e}^{-\mathrm{j}\kappa r}\left[1-\mathrm{j}\kappa\left(r'-r\right)\right],\end{aligned}\tag{24}$$

is similar to the approximation of the electric dipole [14], which yields

$$\boldsymbol{A}(r) = \frac{\mu_0 \boldsymbol{I}}{4\pi}\mathrm{e}^{-\mathrm{j}\kappa r}\left[\left(1+\mathrm{j}\kappa r\right)\oint_\ell \frac{\mathrm{d}l'}{\rho'} - \mathrm{j}\kappa\oint_\ell \mathrm{d}l'\right]\boldsymbol{u}_\gamma.\tag{25}$$

For the purposes here, the second integral in (25) is zero since all it indicates is to continue moving the observation point around the circle to the starting point of integration. Therefore, evaluation of the first integral in (25) yields by vector identity

$$\oint_\ell b\,dl' = \int_{\Delta s}\left(\boldsymbol{u}_{\boldsymbol{n}}\times\nabla b\right)\cdot \mathrm{d}s,\tag{26}$$

to convert to a surface integral. The scalar b is equal to the inverse of the amplitude $(1/r')$, the unit vector $\boldsymbol{u}_{\boldsymbol{n}} = \boldsymbol{u}_z$, since the antenna is restricted to the $x-y$ plane and projecting along z, illustrated in Fig. 3. The decomposition

$$\begin{aligned}\oint_\ell \frac{\mathrm{d}l'}{r'} &= \int_{\Delta s}\left(\boldsymbol{u}_z\times\nabla\frac{1}{r'}\right)\cdot\boldsymbol{u}_\gamma \mathrm{d}s,\\&= -\int_{\Delta s}\left(\boldsymbol{u}_z\times\nabla\frac{\boldsymbol{u}_{r'}}{(r')^2}\right)\cdot\boldsymbol{u}_\gamma \mathrm{d}s,\end{aligned}\tag{27}$$

yields πa^2. Since it is expected the shape be homogenous and elliptical given the antenna geometry, the representation in spherical coordinates is the vector relation

$$\boldsymbol{u}_z\times\boldsymbol{u}_r = \sin\theta\boldsymbol{u}_\gamma,\tag{28}$$

transforming to

$$\oint_\ell \frac{\mathrm{d}l'}{r'} = \frac{\pi a^2}{r^2}\sin\theta,\tag{29}$$

yields

$$\boldsymbol{A}(\boldsymbol{r}) \simeq \mathrm{j}\frac{\mu_0\left(I\pi a^2\right)\kappa}{4\pi}\frac{\mathrm{e}^{-\mathrm{j}\kappa r}}{r}\sin\theta\boldsymbol{u}_\gamma,\tag{30}$$

suggesting there are disturbances between the coupled-mode of the antenna, the boundary of its field, and the potential at the interface to free-space in the neighbourhood due to the magnitude of local forces. Such forces contained in the potential field are manifested as an additional voltage in the circuit, in differentiated time, $\tau = \alpha t$, over a time interval, as

$$V(\alpha,\,\tau) = \frac{1}{\alpha C}\begin{cases}e^{-(G/\alpha C)\tau}, & 0<\tau<t\\ e^{-(G/\alpha C)\tau} - e^{-(G/\alpha C)(\tau-t)}, & t<\tau\end{cases},\tag{31}$$

where α is the factor of stray between one area of time in one moving field and another. We only consider two areas in this paper, although more could be present. The value of (31) describes forward and reverse contributions of the forces, generically in terms of capacitance, C, conductance, G, and voltage, V, of the circuit

$$C\frac{\mathrm{d}V}{\mathrm{d}t} + GV = I_0(t),\tag{32}$$

and

$$\alpha C\frac{\mathrm{d}V}{\mathrm{d}\tau} + GV = I_0(\tau),\tag{33}$$

respectively.

4 Simulation using the FEM tool chain

According to [16], the energy balance equation including the forcive influence within the electromagnetic field is expressed as

$$\int_{\Omega}\left(\sigma_0 \boldsymbol{E}\frac{\partial \boldsymbol{E}}{\partial t}+\mu_0 \boldsymbol{H}\frac{\partial \boldsymbol{H}}{\partial t}\right)d\Omega+\int_{\Omega}\frac{|\boldsymbol{J}|^2}{\sigma}d\Omega - \int_{\Omega}\boldsymbol{E}_i \boldsymbol{J}d\Omega+\oint_{\Gamma}F_{\mathrm{R}}(\boldsymbol{E}\times\boldsymbol{H})d\Gamma=0. \quad (34)$$

In (34), the first integral accounts for the rate of change of energy density of the electromagnetic field in the volume, Ω, given the distribution of the field from (20), the second integral considers the dissipated energy (the Joule heat), the third integral includes the injected energy by the source voltage, and the last integral stands for the intensity of energy flow through the surface Γ, the surface integral of the Poynting vector, with a directional force coefficient from (18). By applying the energy conversion theorem to the present quasi static problem formulation with sinusoidal sources on (34), we can set the total magnetic field energy, W_{T}, inside the volume Ω equal to the stored energies expressed by the circuit elements L_1, L_2, and forward mutual inductance, M_{12}, as

$$W_{\mathrm{T}}=\int_{\Omega}\frac{\mu_0 H^2}{2}\mathrm{d}\Omega = \frac{L_1 I_1^2}{2}+M_{12}I_1 I_2+\frac{L_2 I_2^2}{2}. \quad (35)$$

The same approach could be applied to determine the power loss of the copper windings which is equal to the dissipated energy (the Joule heat) and the stored electric energy expressed by the parasitic capacitors C_1, C_2, C_{12}, as well as the forces in the inductors.To verify the fundamental principle of power transfer utilised for NFC communication systems, we compare the results of (35) gained by FEM simulation with measurements. A proper simulation of the present radio frequency identification (RFID) problem can be carried out with the *ElmerFEM Physics Solver* [17]. This open source package involves a three-dimensional FEM based on a formulation [18] for the magnetic vector potential $\boldsymbol{A}$ and the electric scalar $\boldsymbol{V}$ for solving Maxwell's equations in order to derive the approximated values of (34). *FastHenry* [19], a PEEC-based solver [20], is used as second solver to determine L_1, L_2, and M_{12} for comparison.The details of the simulation setup for NFC and RFID related problems are described in [21]. Here, we consider L_1, L_2, and M_{12} as the unknowns and by solving (35) as a linear 3×3 equation system, where $W_{\mathrm{T}}(I_1, I_2)$ is the total magnetic field energy of the volume Ω introduced by the coil currents I_1 and I_2, then we obtain the numbers for the coupled scenario according to Fig. 2.

Fig. 4 shows a meshed scenario of an ID-1 sized credit-card pair with 10 mm vertical displacement. The antenna setup is surrounded by a $50\times50\times50$ cm air cube defining the volume Ω. The magnetic field on the boundary surfaces of this air cube is set to zero. This means that no energy is transferred out of the modelling setup and insists the fourth integral of (34) to be zero. This is a purposeful simplification which effects the final numerical results of the total magnetic energy W_{T}, differentiated from true result can be neglected.

Fig. 5 shows the comparison between calculated [7], measured, and simulated values of the coupling factor against *z*-dimension displacement of two credit-card (ID-1) sized antennas (class 1 antenna size according to [2]) in the coaxial coupling scenario. It is noted that the different methods are in excellent agreement and demonstrates that the magnetic energy balance equation in tandem with field mapping presented in this paper is a valid approach to determine the contactless power transmission characteristic of NFC antennas. In order to transfer power delivered by a carrier at designated frequencies, special methods are required [22, 23].

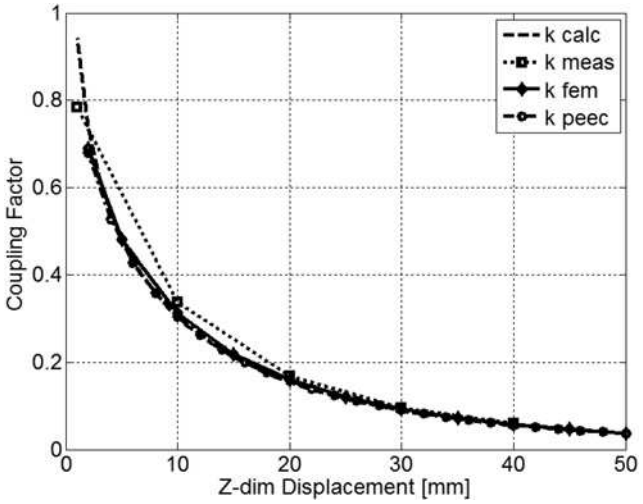

Fig. 5 *Shows the comparison between calculated (k calc), measured (k meas), and simulated (k fem, k peec) coupling factor against the z-dimension displacement of the class 1–class 1 antenna coupling scenarios*

5 Testing NFC reader power

This section will discuss the amount of transmitted power in NFC and Proximity system operation. Contactless testing of NFC interfaces, Proximity cards and readers, or Vicinity tags is done at the air interface, where the part opposite of the device under test emulates a reader or a card. There are three test environments relevant for 13.56 MHz contactless technology, specified by ISO/IEC in the context of Proximity and Vicinity cards, by EMVCo specifically for payment applications, and by the NFC Forum for NFC devices. In the Proximity Test Standard [24] and in NFC [4], the concept for measurement of power transfer or alternating *H*-field at the air interface takes into account the loading of the card resonant antenna circuit on the reader resonant antenna circuit, similar to a loaded transformer model. An emulation of a contactless card resonant antenna circuit is used as measurement device, either called ISO/IEC Reference PICC for Proximity, or NFC Forum Listener. These devices are available with different antenna sizes, e.g. Class 1–6 for the ISO/IEC Ref. PICC, or as NFC Forum Listener 1, 3, and 6, to cover the existing variety of antenna sizes for NFC devices and Proximity cards, which will all have different coupling factors. The first and originally the only antenna size is Class 1 as shown in Fig. 1, which is most important. In our example we will follow the NFC Forum Reader Power specification for Class 1, summarised in Table 1.

In addition to the test environment, there are also test methods defined, which are used to verify contactless system properties according to Standard specifications. Contactless reader power transmission may be the first and elementary aspect here. According to the test concepts, a reader must exceed a minimum alternating *H*-field (or a minimum voltage on a resistor of the NFC Forum Listener) and must not exceed a maximum alternating *H*-field (or a maximum voltage on a resistor of the NFC Forum Listener) in the operational volume, for parallel antenna planes. As all these systems use resonant antenna coils on reader and card side, also the testing is done with NFC Forum Listener antenna circuit adjusted to 13.56 MHz resonance frequency.

Table 1 NFC Forum Reader power requirements for measurement with listeners 1, 3, and 6

	Listener	1	3	6
H_{MIN}	R_{LOAD} in Ω	820	820	820
	U_{MEAS} in V_{DC}	4.10	3.14	3.79
H_{MAX}	R_{LOAD} in Ω	82	82	82
	U_{MEAS} in V_{DC}	2.85	2.50	2.23

The quality factor of the Listener is adjusted with the load resistor. The maximum H-field condition is tested with a lower Q-factor using an 82 Ω load resistor, following a full-bridge rectifier. The specified voltage for Listener 1 of 2.85 volts DC corresponds to a maximum power of ∼100 mW, accordingly

$$P(@H_{\mathrm{MAX}}) = \frac{2.85\ \mathrm{V}_{\mathrm{DC}}^2}{82\ \Omega} \cong 99\ \mathrm{mW}. \tag{36}$$

The minimum H-field condition is tested with a higher Q-factor, using an 820 Ω load resistor. The specified voltage for Listener 1 of 4.1 volts DC corresponds to a minimum power of 20 mW, accordingly

$$P(@H_{\mathrm{MIN}}) = \frac{4.1\ \mathrm{V}_{\mathrm{DC}}^2}{820\ \Omega} \cong 20\ \mathrm{mW}. \tag{37}$$

Even though in this test condition less effective power is transmitted, the higher Q means more reactive current in the Listener coil. This stands for a higher 'Card loading' to the reader, in the wording of the standard. This 'loading' aspect is also specified and may range from almost no effect for an open card antenna coil, up to a maximum value, which is emulated by the Listener for the minimum reader power test case.

What is the maximum effective power that may be transmitted in an NFC or Proximity system? One might guess, 100 mW, as indicated above by the maximum H-field condition. This is, however, not the case. A contactless reader may be built in such way, that it is not influenced by Card loading. Adjusted in a way that it will just pass the maximum H-field test condition, a Card tuned to resonance at 13.56 MHz and the highest allowed Q-factor (according to the minimum H-field test condition) may receive much more power. As the Proximity Test Standard PCD1 antenna arrangement shows only low impact from loading (<7% according Table 2 in [25]), we can refer the NFC Forum reader power specification to the Proximity Test Standard by a measurement series.

As Fig. 6 shows, the NFC Forum Listener 1 definition for minimum and maximum reader power corresponds well to the Proximity Test Standard definition for Class 1. In the case of maximum loading, the result is 27.3 V (DC) over the 820 Ω shunt-load resistor, which corresponds to about 900 mW loss of power. That is the level of heat dissipation which NFC interfaces have to be designed for. This quantity of power could be used for other applications such as wireless charging.

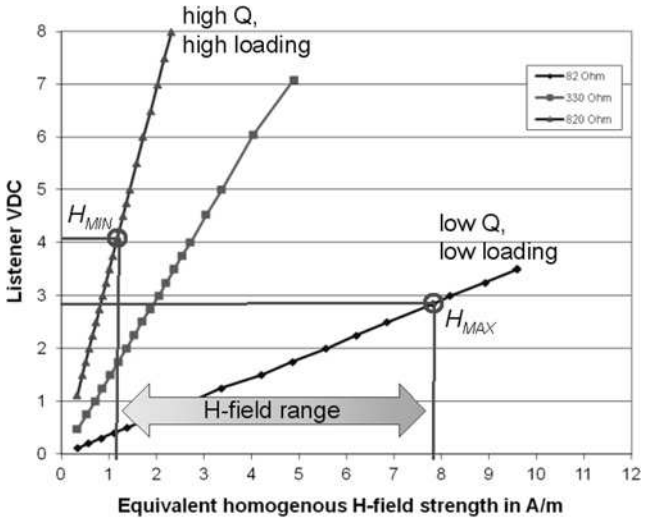

Fig. 6 *NFC Forum Listener 1 output voltage as function of ISO/IEC specified equivalent homogenous 13.56 MHz alternating H-field*

6 Conclusions

This paper explored theoretical concepts and frame conditions to improve the NFC solution development process supported by an experimental setup. The paper presented a novel computational model using forces and couples to map the dynamics of energy oscillating between the primary and secondary circuits, as a characteristic of the oscillator circuitry, where reactive forces appear as voltages in differential time. The authors used the theory in terms of kinetic energy for mapping and calculating field quantities to maximise contactless power transmission by inductive loop antennas in the reactive near-field. The authors then presented a solution which agreed with the theory to calculate the total energy and used an FEM simulation technique for NFC and RFID.

The theory only implicitly addresses the magnetic potential, $\boldsymbol{A}$, as a function of $\boldsymbol{B}$, when determining the role of energy exchange in the flux pattern. However, we proffer our methodology as a contrast to the widely-accepted Biot–Savart method. It is expected in a future work that an analysis of $\boldsymbol{A}$ would show enhancement of the field wherein greater exchange of both flux and energy between the coils is realised. It is also proposed that quantising the field in such a manner, closely following the behaviour of the circuit, yields insights where potential fields lie and energy exchange takes place in an antenna within a given geometry.

It was the intention of the authors to undertake a deeper examination of the role of the coupling factor and what constitutes 'transferred power' between two coupled coils. By doing this, we propose to make a novel contribution by demonstrating such an effort will aid development of RFID and other wireless power technologies as implementation is integrated into smaller packages where such tiny components using coupled modes only rely on micro, nano, or pico-scaled quantities of power.

Future work could consider the surface integral of the Poynting vector along antenna surface boundaries as the basis for FEM simulation frameworks to represent the contiguous field in terms of an object comprised of potential fields and reactive forces. With these results a direct solution could be shown for the coupling factor combined with the forces manifesting in parametric values of $\boldsymbol{A}$, dependent upon circuital parameters. Research could be extended to include skin-effect and eddy current losses which are a dominant source of power transmission degradation. Finally, further experiments and circuital models could be proposed which demonstrate forces at the interface of an antenna at free-space to perform useful work for a variety of applications.

7 References

1 ISO/IEC 10536, Identification cards – Contactless integrated circuit cards – Close coupling cards – part 1, 2, 3, 4, ISO, Geneva, Switzerland, 1995–2000
2 ISO/IEC 14443:2011(E), Identification cards – Contactless integrated circuit cards – Proximity cards – part 1, 2, 3 and 4, ISO, Geneva, Switzerland, 2nd ed. 2008–2011
3 ISO/IEC 15693: 2006(E), Identification cards – Contactless integrated circuit cards – Vicinity cards – part 1, 2, 3, Geneva, Switzerland, 2006
4 NFC Forum (www.nfc-forum.org/specs/), NFC Analogue Specification, Revision Draft 0.38, Jun. 2011
5 Maxwell, J.C.: 'A treatise on electricity and magnetism' (Clarendon Press, Oxford, 1891, 3rd edn.), vol. 1
6 Haus, H.A., Huang, W.: 'Coupled mode theory'. Proc. IEEE, 1991, vol. 79, no. 10, pp. 1505–1518
7 Neumann, F.E.: 'Allgemeine Gesetze der inducirten elektrischen Ströme', Abhandlungen der Königlichen Akademie der Wissenschaften zu Berlin, 1845, Seiten 1–87
8 Grover, F.W.: 'Inductance calculations working formulas and tables' (Dover Publications, Inc., New York, 1946)
9 Hackl, S., Lanschützer, C., Raggam, P., *et al.*: 'A novel method for determining the mutual inductance for 13.56 MHz RFID systems'. Sixth Int. Symp. on Communication Systems, Networks and Digital Signal Processing, Graz, July 2008, pp. 120–124
10 Fotopoulou, K., Flynn, B.F.: 'Optimum antenna coil structure for inductive powering of passive RFID tags'. Int. Conf on RFID, Grapevine, March 2007, pp. 72–77

11 Larmor, J.: 'On a dynamical theory of the electric and luminiferous medium, theory of electrons', *Philos. Trans. R. Soc.*, 1895, pp. 719–822
12 Kraus, J.D.: 'Antennas for all applications' (McGraw-Hill, Boston, 2001, 3rd edn.)
13 Tucker, C.A.: 'Magnetic resonant modes in a wireless-powered circuit'. 19th Telecommunications Forum TELFOR, 2011, pp. 977–980
14 Fano, R., Chu, L., Alder, R.: 'Electromagnetic fields, energy, and forces' (John Wiley & Sons, New York, 1969)
15 Georgieva, N., Yamashita, E.: 'Time-domain vector-potential analysis of transmission-line problems', *IEEE Trans. Microw. Theory Tech.*, 1998, **46.4**, pp. 404–410
16 Inan, U.S., Inan, A.S.: 'Engineering electromagnetics' (Addison-Wesley, Boston,, 1999)
17 ElmerFEM, Open Source Finite Element Software for Multiphysical Problems. Available at: http://www.csc.fi/english/pages/elmer
18 Biro, O., Preis, K.: 'On the use of the magnetic vector potential in the finite element analysis of three-dimensional eddy currents', *IEEE Trans. Magn.*, 1989, pp. 3145–3159
19 FastHenry M.I.T. source code distribution. Available at: http://www.rle.mit.edu/cpg/research_codes.htm
20 Kamon, M., Tsuk, M.J., White, J.K.: 'FastHenry: a multipole-accelerated 3-D inductance extraction program', *IEEE Trans. Microw. Theory Tech.1 of 2*, 1994, **42**, (9), pp. 1750–1758
21 Muehlmann, U., Gebhart, M., Wobak, M.: 'Mutual coupling modeling of NFC antennas by using open-source CAD/FEM tools'. IEEE RFID-TA, 2012, pp. 393–397
22 Schober, A., Ciacci, M., Gebhart, M.: 'An NFC air interface coupling model for contactless system performance estimation'. 12th Int. Conf. on Telecommunications ConTEL (IEEE), June 2013, Zagreb, Croatia, pp. 243–250
23 Manzi, G.: 'EMV contactless payment systems based on AS3911 overview and system simulations'. CST European User Conf. 2012, Mannheim, May 23–25, 2012
24 ISO/IEC 10373-6, Identification cards – test methods – part 6: 'Proximity Cards' (ISO, Geneva, Switzerland, 2011, 2nd edn.)
25 Gebhart, M.: 'Analytical considerations for an ISO/IEC14443 compliant smartcard transponder'. 11th Int. Conf. on Telecommunications ConTEL (IEEE), Graz, Austria, June 2011, pp. 9–16
26 Tucker, C.A., Warwick, K., Holderbaum, W.: 'A contribution to the wireless transmission of power', *Int. J. Electr. Power Energy Syst.*, 2013, **47**, pp. 235–242
27 Tucker, C.A.: 'Power transfer in velocity-vortex acceleration', *Int. J. Identif. Model. Control*, 2014, **21**, (4)
28 Wireless power consortium, system description wireless power transfer, volume 1: low power, part 1: interface definition, version 1.1.1. Available at: http://www.wirelesspowerconsortium.com, July 2012
29 Alliance for wireless power, A4WP wireless power transfer system baseline system specification, final approved specification. Available at: http://www.rezence.com/, January 2, 2013